Microwave Characterization and Modeling of GaAs/AlGaAs Heterojunction Bipolar Transistors

Rainee N. Simons and Robert R. Romanofsky
Lewis Research Center
Cleveland, Ohio

NASA

MICROWAVE CHARACTERIZATION AND MODELING OF GaAs/AlGaAs

HETEROJUNCTION BIPOLAR TRANSISTORS

Rainee N. Simons and Robert R. Romanofsky
National Aeronautics and Space Administration
Lewis Research Center
Cleveland, Ohio 44135

SUMMARY

The characterization and modeling of a microwave GaAs/AlGaAs heterojunction Bipolar Transistor (HBT) are discussed. The de-embedded scattering parameters are used to derive a small signal lumped element equivalent circuit model using EEsof's "Touchstone" software package. Each element in the equivalent circuit model is shown to have its origin within the device. The model shows good agreement between the measured and modeled scattering parameters over a wide range of bias currents. Further, the MAG and $|h_{21}|$ calculated from the measured data and the MAG and $|h_{21}|$ predicted by the model are also in good agreement. Consequently the model should also be capable of predicting the f_{max} and f_T of other HBTs.

INTRODUCTION

In conventional GaAs Metal Semiconductor Field Effect Transistor (MESFET) and GaAs/AlGaAs High Electron Mobility Transistor (HEMT) devices, current conduction is parallel to the surface and hence the device speed tends to be constrained by limitations of the lithography process which defines the channel length. On the other hand, Heterojunction Bipolar Transistor (HBT) devices have potential for much higher speed since in these devices the electrons travel in a direction perpendicular to the epitaxially grown layers whose thickness can be made much smaller than the horizontal channel dimensions. Since current conduction is in the vertical direction, the HBTs are also capable of handling a much higher current density and consequently much higher power densities. Furthermore, HBTs should be better suited to high-speed digital applications where consistent turn-on voltage is an important requirement. In an HBT, this threshold is determined almost exclusively by the bandgap of the semiconductor in the base region, whereas for a FET device it depends on doping concentration and channel thickness which are process dependent. In addition to the above advantages, HBTs possess higher transconductance and better impedance matching characteristics when compared to FET devices. Typically, input and output impedances of the HBTs tend to be closer to 50 Ω (refs. 1 and 2).

In this paper, the characterization and modeling of a TRW microwave NPN GaAs/AlGaAs HBT are discussed. Potential applications include higher power and higher density monolithic microwave integrated circuits (MMICs).

DEVICE DESCRIPTION

The topology of the measured emitter-up NPN HBT device fabricated at TRW, Redondo Beach, California is shown in figure 1. The device was fabricated

using MBE techniques and includes a linearly graded aluminum composition at the emitter base interface. The transistor has four emitter fingers, each finger having dimensions of 3 by 40 μm. The base finger dimensions are 3.5 by 40 μm. The gaps between the emitter and base fingers are approximately 1.5 to 1.75 μm. The size of the bonding pads are approximately 100 by 100 μm. A detailed description of the basic processing parameters of the device can be found in reference 2.

MEASUREMENT AND CHARACTERIZATION

The transistor chip was mounted on a 3/8 by 3/8 in. 25 mil thick alumina carrier and wire bonded to 50 Ω coplanar waveguide (CPW) in a common emitter configuration. The base and collector dc voltage was supplied through two 50 Ω coaxial bias tees. A CPW calibration kit consisting of a 50 Ω through, short, offset, and open circuit on similar substrates was used to de-embed the scattering parameters. Figures 2(a) and (b) show the design technique coplanar waveguide test fixture and the calibration kit respectively. Full two-port scattering parameter measurements from 0.5 to 8.5 GHz were performed using an HP-8510 automatic network analyzer. The collector voltage V_{CE} was held fixed at 5.0 V. The base current was varied in discrete increments with concommitant increase in the collector current from 2 to 35 mA. The corresponding measured scattering parameters are tabulated in tables I(a) to I(f) for six bias conditions. The common emitter dc current gain (h_{FE}) as determined from a plot of collector current versus the base current is 55 and is illustrated in figure 3.

DEVICE MODELING AND NUMERICAL RESULTS

Each element in the equivalent circuit has its origin within the device as shown in figure 4. A common emitter small signal lumped element bias dependent equivalent circuit model that is used to fit the de-embedded scattering parameters is illustrated in figure 5. In obtaining this model the conventional bipolar transistor equivalent circuit was modified to more accurately represent the interdigitated geometry of the measured HBT. The base of the transistor can be modeled as a distributed RC network due to the base resistance and the base-collector capacitance. R_{B2} includes base contact resistance and the resistance of the semiconductor region between the base contact and the emitter stripe. The resistance R_{B1} is due to the semiconductor resistance in the active base region. The total base resistance contributes significantly to limiting the upper frequency of operation of the HBT. Capacitance C_1 arises from the extrinsic base region whereas C_c is due to the active base region. R_E and C_E are the resistance and capacitance associated with the forward biased base-emitter junction. The resistance R_3 and R_{EC} are the collector and emitter contact resistances respectively. R_{EC} tends to be a sensitive parameter especially in determining the input reflection coefficient. C_2 and C_{CE} are the collector and emitter bonding pad capacitances respectively. R_C is the collector resistance shunted across the models dependent current source and tends to be relatively large. Inductances L_B, L_C, and L_E represent the effect of the bond wires and parasitics which cannot be mathematically removed during the de-embedding procedure.

The circuit was optimized using EEsof's "Touchstone" software package (ref. 3). Table II lists the optimized equivalent circuit element values for

2

six bias conditions. The corresponding modeled scattering parameters are tabulated in tables III(a) to III(f). A good overall indication of the quality of the model is the match between the maximum available power gain (MAG) and the current gain ($|h_{21}|$) calculated from the measured data and the MAG and 'h_{21}' predicted by the model since all the four scattering parameters are required. Plots of measured and modeled MAG, $|h_{21}|$, and the scattering parameters are shown in figures 6 to 11. In these figures and in tables IV and V the measured and modeled parameters are denoted as "TRW" and "NASAHBT" respectively. Good agreement is observed between the measured and modeled scattering parameters. The measured and modeled maximum stable gain (MSG) or MAG as well as the stability factor (K) are listed in tables IV(a) to IV(f). The measured and modeled $|h_{21}|$ is listed in tables V(a) to V(f). Circuit optimization was continued until an error function of 0.05 or better was obtained. This resulted in a close agreement between the measured and modeled MAG and $|h_{21}|$.

The maximum frequency of oscillation (f_{max}) was determined by extrapolating the MAG to the 0 dB gain axis at -6 dB/octave. Similarly, by extrapolating the $|h_{21}|$ curve the unity current gain cutoff frequency (f_T) could be predicted. These results are summarized in figure 12 which shows f_{max} and f_T as a function of collector current. It is to be observed that both f_{max} and f_T increase in proportion to I_C initially and then tend to saturate beyond some current for a fixed V_{CE}. Further, it is also interesting to note that for I_C below 9.75 mA f_T actually falls below f_{max}. A maximum f_T of 11.4 GHz was observed for I_C equal to 35 mA which corresponds to an effective emitter to collector transit time of 14 psec. The corresponding f_{max} at I_C = 35 mA was 9 GHz which results in an equivalent base-resistance collector-capacitance time constant $(R_{B1}C_C)_{eff}$ of 5.6 psec.

CONCLUSION

A small signal lumped element equivalent circuit model for a microwave GaAs/AlGaAs HBT was derived from the de-embedded scattering parameters using EEsof's "Touchstone" software. Each element in the equivalent circuit is shown to have its origin within the device. The model shows good agreement between the measured and modeled scattering parameters over a wide range of bias currents. Further, the MAG and $|h_{21}|$ calculated from the measured data and the MAG and $|h_{21}|$ predicted by the model are also in good agreement. Consequently the model is suitable for predicting the performance of other HBTs.

ACKNOWLEDGMENT

REFERENCES

1. Kroemer, H.: Heterostructure Bipolar Transistors and Integrated Circuits. Proc. IEEE, vol. 70, no. 1, Jan. 1982, pp. 13-25.

2. Kim, M.E., et al.: GaAs/Al$_{0.3}$Ga$_{0.7}$As Heterojunction Bipolar Transistors
   and Integrated Circuits with High Current Gain for Small Device Geometries.
   IEEE Gallium Arsenide Integrated Circuit Symposium, IEEE, 1986, pp. 162-166.

3. EEsof Touchstone User's Manual. EEsof Inc., 1986, pp. EL-1.

TABLE I. - MEASURED SCATTERING PARAMETERS

[V_{CE} = 5.0 V.]

(a) I_B = 0.053 mA, I_C = 2.0 mA

FREQ-GHZ	DB[S11] TRW	ANG[S11] TRW	DB[S21] TRW	ANG[S21] TRW	DB[S12] TRW	ANG[S12] TRW	DB[S22] TRW	ANG[S22] TRW
0.500000	-3.092	-78.019	12.319	127.620	-19.438	45.840	-2.549	-31.122
1.00000	-4.026	-118.760	8.776	102.980	-17.170	28.950	-4.816	-42.363
1.50000	-4.224	-139.090	6.102	87.947	-16.628	22.054	-5.958	-48.020
2.00000	-4.380	-152.390	4.069	76.461	-16.421	18.182	-6.481	-53.976
2.50000	-4.302	-161.280	2.574	67.503	-16.404	17.132	-6.655	-58.634
3.00000	-4.673	-170.010	1.273	58.314	-16.375	17.629	-6.794	-64.704
3.50000	-4.395	-176.490	0.231	50.799	-16.295	18.880	-6.888	-70.825
4.00000	-4.310	177.430	-0.673	43.881	-16.159	20.374	-6.903	-77.053
4.50000	-4.279	172.085	-1.354	37.979	-15.928	23.424	-6.954	-82.941
5.00000	-4.249	166.740	-2.093	32.077	-15.704	26.473	-7.005	-88.830

(b) I_B = 0.0915 mA, I_C = 4.0 mA

FREQ-GHZ	DB[S11] TRW	ANG[S11] TRW	DB[S21] TRW	ANG[S21] TRW	DB[S12] TRW	ANG[S12] TRW	DB[S22] TRW	ANG[S22] TRW
0.500000	-4.027	-93.208	15.892	122.320	-20.910	42.333	-4.098	-43.956
1.00000	-4.625	-132.020	11.688	99.992	-19.083	30.199	-7.458	-57.469
1.50000	-4.636	-149.400	8.787	87.075	-18.444	27.319	-9.199	-63.052
2.00000	-4.701	-160.700	6.635	77.224	-17.942	26.506	-10.025	-68.395
2.50000	-4.694	-160.540	6.637	77.189	-17.948	26.555	-10.017	-68.376
3.00000	-4.936	-176.060	3.713	61.264	-17.065	29.085	-10.515	-76.812
3.50000	-4.624	178.270	2.625	54.473	-16.529	30.328	-10.613	-81.999
4.00000	-4.550	173.160	1.678	48.112	-15.997	31.174	-10.586	-87.175
4.50000	-4.521	168.540	0.926	42.653	-15.581	32.585	-10.652	-91.708
5.00000	-4.462	163.250	0.214	36.693	-14.959	34.048	-10.667	-96.886
5.50000	-4.485	158.970	-0.487	31.226	-14.261	34.932	-10.752	-102.640
6.00000	-4.510	153.430	-1.177	26.912	-13.627	35.343	-10.895	-108.590

TABLE I. - Continued.

(c) I_B = 0.193 mA, I_C = 9.25 mA

FREQ-GHZ	DB[S11] TRW	ANG[S11] TRW	DB[S21] TRW	ANG[S21] TRW	DB[S12] TRW	ANG[S12] TRW	DB[S22] TRW	ANG[S22] TRW
0.500000	-4.626	-115.300	18.600	113.620	-22.883	41.059	-5.346	-60.993
1.00000	-5.770	-143.480	13.854	97.131	-21.230	34.913	-9.289	-83.828
1.50000	-5.328	-157.600	10.861	85.939	-20.211	36.061	-11.476	-93.398
2.00000	-5.016	-167.720	8.571	77.048	-19.202	37.672	-12.781	-101.970
2.50000	-5.024	-174.140	6.991	69.330	-18.282	39.319	-13.763	-106.680
3.00000	-5.099	179.400	5.587	62.420	-17.346	40.464	-14.213	-111.150
3.50000	-4.929	174.050	4.407	56.246	-16.449	40.910	-14.502	-115.060
4.00000	-4.917	169.810	3.449	51.025	-15.648	40.704	-14.621	-119.290
4.50000	-4.905	165.380	2.622	45.461	-14.974	40.401	-14.886	-122.710
5.00000	-4.796	161.090	1.893	40.001	-14.198	40.421	-14.977	-125.780
5.50000	-4.654	156.870	1.198	35.965	-13.528	40.301	-15.213	-128.980
6.00000	-4.573	153.360	0.554	31.273	-12.912	38.949	-15.473	-133.290

(d) I_B = 0.321 mA, I_C = 17.0 mA

FREQ-GHZ	DB[S11] TRW	ANG[S11] TRW	DB[S21] TRW	ANG[S21] TRW	DB[S12] TRW	ANG[S12] TRW	DB[S22] TRW	ANG[S22] TRW
0.500000	-5.380	-129.910	19.921	109.510	-24.730	39.404	-7.941	-83.136
1.00000	-5.140	-154.640	14.895	93.201	-22.919	40.457	-11.962	-106.520
1.50000	-5.023	-165.800	11.731	84.104	-21.384	43.859	-13.718	-120.670
2.00000	-5.011	-173.200	9.397	76.403	-19.901	46.244	-14.712	-130.390
2.50000	-5.022	-178.450	7.734	70.004	-18.664	47.722	-15.293	-135.640
3.00000	-5.367	175.810	6.314	63.408	-17.472	48.182	-15.642	-140.360
3.50000	-4.891	171.380	5.150	57.978	-16.312	47.497	-15.894	-144.620
4.00000	-4.902	167.730	4.197	52.969	-15.392	46.114	-15.986	-148.950
4.50000	-4.932	163.210	3.442	47.649	-16.010	45.217	-16.252	-152.730
5.00000	-4.870	158.660	2.646	42.148	-13.823	44.118	-16.388	-157.090
5.50000	-4.826	154.290	2.001	37.355	-13.031	42.551	-16.686	-161.800
6.00000	-4.919	149.200	1.454	33.246	-12.340	40.799	-16.785	-166.940
6.50000	-4.786	146.340	0.960	28.729	-11.737	38.846	-16.794	-173.670
7.00000	-4.777	142.330	0.467	23.847	-11.277	36.534	-16.762	177.500
7.50000	-4.971	139.390	0.104	22.350	-10.932	37.017	-18.269	173.020
8.00000	-4.694	136.840	-0.101	16.539	-10.026	34.365	-16.755	174.340

5

TABLE I. - Concluded.

(e) I_B = 0.457 mA, I_C = 25.0 mA

FREQ-GHZ	DB[S11] TRW	ANG[S11] TRW	DB[S21] TRW	ANG[S21] TRW	DB[S12] TRW	ANG[S12] TRW	DB[S22] TRW	ANG[S22] TRW
0.500000	-5.501	-136.970	20.421	106.890	-25.655	40.336	-8.642	-93.694
1.00000	-5.194	-158.670	15.249	91.725	-23.538	43.716	-12.245	-119.560
1.50000	-5.074	-168.520	12.047	83.329	-21.728	47.866	-13.578	-134.280
2.00000	-5.032	-175.130	9.712	75.955	-20.035	49.857	-14.318	-143.930
2.50000	-5.069	-179.880	8.020	69.916	-18.639	50.909	-14.845	-149.550
3.00000	-5.375	174.470	6.615	63.476	-17.364	51.014	-15.098	-154.000
3.50000	-4.924	170.160	5.413	58.342	-16.150	49.749	-15.271	-158.190
4.00000	-4.935	166.950	4.477	53.372	-15.186	48.115	-15.490	-162.240
4.50000	-4.917	162.300	3.669	48.213	-14.428	46.750	-15.715	-166.650
5.00000	-4.887	158.160	2.933	42.955	-13.597	45.428	-15.848	-171.160
5.50000	-4.851	153.620	2.284	38.282	-12.777	43.605	-16.082	-175.730
6.00000	-4.948	148.550	1.708	34.139	-12.097	41.579	-16.282	-179.070
6.50000	-4.818	145.640	1.229	29.666	-11.507	39.407	-16.242	172.470
7.00000	-4.774	142.290	0.764	25.470	-11.030	37.160	-16.055	164.760
7.50000	-5.073	139.190	0.338	23.297	-10.701	37.333	-17.438	158.440
8.00000	-4.710	136.160	0.206	17.559	-9.817	34.320	-16.343	160.520
8.50000	-4.424	132.900	-0.393	11.842	-9.022	32.824	-14.017	158.810

(f) I_B = 0.6536 mA, I_C = 35.0 mA

FREQ-GHZ	DB[S11] TRW	ANG[S11] TRW	DB[S21] TRW	ANG[S21] TRW	DB[S12] TRW	ANG[S12] TRW	DB[S22] TRW	ANG[S22] TRW
0.500000	-5.637	-141.840	20.686	105.210	-26.318	41.869	-9.089	-100.510
1.00000	-5.305	-161.450	15.435	90.832	-23.959	46.512	-12.294	-127.420
1.50000	-5.155	-170.450	12.210	82.800	-21.943	50.783	-13.354	-141.930
2.00000	-5.124	-176.590	9.863	75.711	-20.093	52.594	-13.944	-151.250
2.50000	-5.140	-178.960	8.168	69.800	-18.647	53.171	-14.386	-156.790
3.00000	-5.441	-173.440	6.764	63.421	-17.290	52.944	-14.624	-161.260
3.50000	-5.013	169.240	5.565	58.374	-16.046	51.299	-14.832	-165.510
4.00000	-4.981	165.900	4.631	53.642	-15.081	49.315	-15.002	-169.800
4.50000	-5.020	161.580	3.820	48.367	-14.297	47.733	-15.243	-174.030
5.00000	-4.993	157.370	3.072	43.241	-13.469	46.230	-15.372	-178.590
5.50000	-4.961	153.030	2.410	38.581	-12.645	44.103	-15.636	-176.710
6.00000	-5.009	148.000	1.856	34.523	-11.979	41.973	-15.782	171.320
6.50000	-4.901	145.080	1.369	30.054	-11.380	39.558	-15.741	165.010
7.00000	-4.851	141.310	0.892	25.764	-10.917	37.154	-15.520	157.690
7.50000	-5.111	138.140	0.541	23.998	-10.567	37.157	-16.773	150.550
8.00000	-4.863	135.570	0.360	18.066	-9.721	34.092	-15.930	153.000
8.50000	-4.498	132.340	-0.272	12.579	-8.971	32.540	-13.893	153.310

TABLE II. - OPTIMIZED COMMON EMITTER SMALL-SIGNAL LUMPED-ELEMENT, EQUIVALENT CIRCUIT MODEL

ELEMENT VALUES

$[V_{CE} = 5.0 \text{ V.}]$

	I_B = 0.053 mA; I_C = 2.0 mA	I_B = 0.0915 mA; I_C = 4.0 mA	I_B = 0.193 mA; I_C = 9.25 mA	I_B = 0.321 mA; I_C = 17.0 mA	I_B = 0.457 mA; I_C = 25.0 mA	I_B = 0.6536 mA; I_C = 35.0 mA
RB1, Ω	8.93203	10.28771	21.71162	34.11475	31.34881	35.0946
RB2, Ω	0.14671	3.49379	0.28315	0.32562	0.46383	0.22044
RC, Ω	4.32×10^6	2.12×10^6	3.48×10^6	3.22×10^6	3.16×10^6	2.38×10^6
RE, Ω	4.111×10^{-5}	6.280×10^{-5}	2.041×10^{-5}	2.563×10^{-5}	2.132×10^{-5}	1.515×10^{-5}
REC, Ω	13.91411	7.99661	4.98334	3.13211	2.56719	2.24090
R3, Ω	1.24249	0.96219	0.86466	0.98836	1.32368	1.03783
C1, pf	0.17716	0.28889	0.25197	0.31314	0.32678	0.24882
C2, pf	0.41004	0.27008	0.32791	0.25454	0.25655	0.31182
CC, pf	5.225×10^{-5}	6.026×10^{-5}	6.333×10^{-5}	6.337×10^{-5}	5.168×10^{-5}	1.989×10^{-5}
CE, pf	0.02323	0.20925	0.17952	0.17480	0.21102	0.21216
CCE, pf	0.02123	0.03574	0.03888	0.01697	0.01244	0.01422
LB, nH	0.29356	0.29356	0.29356	0.29356	0.29356	0.29356
LC, nH	0.05609	0.05609	0.05609	0.05609	0.05609	0.05609
LE, nH	0.04946	0.04946	0.04946	0.04946	0.04946	0.04946
A	0.95371	0.97111	0.98962	0.98852	0.98901	0.98998
T, ps	9.98420	9.90536	3.19025	2.85629	3.63367	4.42523

TABLE III. - MODELED SCATTERING PARAMETERS

[V_{CE} = 5.0 V.]

(a) I_B = 0.053 mA, I_C = 2.0 mA

FREQ-GHZ	DB[S11] NASAHBT	ANG[S11] NASAHBT	DB[S21] NASAHBT	ANG[S21] NASAHBT	DB[S12] NASAHBT	ANG[S12] NASAHBT	DB[S22] NASAHBT	ANG[S22] NASAHBT
0.500000	-3.692	-81.615	12.528	129.374	-18.525	53.435	-2.162	-31.861
1.00000	-4.400	-123.124	8.880	102.718	-15.908	40.071	-4.670	-43.439
1.50000	-4.691	-144.814	6.127	86.605	-14.798	35.921	-6.073	-48.936
2.00000	-4.829	-158.330	4.091	74.767	-13.957	34.483	-6.815	-53.698
2.50000	-4.908	-167.946	2.542	65.157	-13.205	33.711	-7.215	-58.718
3.00000	-4.960	-175.425	1.329	56.975	-12.513	32.938	-7.434	-64.029
3.50000	-4.999	178.400	0.356	49.841	-11.880	31.967	-7.550	-69.501
4.00000	-5.029	173.091	-0.441	43.541	-11.308	30.769	-7.606	-75.005
4.50000	-5.052	168.395	-1.107	37.935	-10.796	29.374	-7.625	-80.447
5.00000	-5.068	164.157	-1.671	32.917	-10.340	27.827	-7.621	-85.761

(b) I_B = 0.0915 mA, I_C = 4.0 mA

FREQ-GHZ	DB[S11] NASAHBT	ANG[S11] NASAHBT	DB[S21] NASAHBT	ANG[S21] NASAHBT	DB[S12] NASAHBT	ANG[S12] NASAHBT	DB[S22] NASAHBT	ANG[S22] NASAHBT
0.500000	-3.925	-97.292	16.102	123.820	-20.197	47.557	-3.467	-44.463
1.00000	-4.410	-136.368	11.770	100.212	-18.155	36.909	-6.952	-58.053
1.50000	-4.570	-155.001	8.730	86.852	-17.170	35.178	-8.841	-63.785
2.00000	-4.641	-166.449	6.507	77.045	-16.321	35.480	-9.800	-68.154
2.50000	-4.683	-174.686	4.799	68.929	-15.512	36.003	-10.244	-72.506
3.00000	-4.713	178.784	3.439	61.829	-14.744	36.233	-10.397	-77.029
3.50000	-4.738	173.281	2.327	55.448	-14.026	36.061	-10.380	-81.657
4.00000	-4.759	168.456	1.400	49.633	-13.365	35.511	-10.264	-86.290
4.50000	-4.778	164.112	0.613	44.295	-12.761	34.643	-10.090	-90.853
5.00000	-4.795	160.131	-0.063	39.373	-12.212	33.522	-9.885	-95.294
5.50000	-4.809	156.438	-0.653	34.823	-11.717	32.207	-9.666	-99.584
6.00000	-4.820	152.981	-1.172	30.609	-11.271	30.747	-9.443	-103.707

(c) I_B = 0.193 mA, I_C = 9.25 mA

FREQ-GHZ	DB[S11] NASAHBT	ANG[S11] NASAHBT	DB[S21] NASAHBT	ANG[S21] NASAHBT	DB[S12] NASAHBT	ANG[S12] NASAHBT	DB[S22] NASAHBT	ANG[S22] NASAHBT
0.500000	-3.591	-114.535	18.811	114.922	-21.163	43.838	-5.600	-63.109
1.00000	-4.182	-148.792	13.751	95.596	-19.235	40.620	-9.735	-80.630
1.50000	-4.349	-164.290	10.492	85.102	-17.780	42.588	-11.675	-89.561
2.00000	-4.429	-173.946	8.156	77.285	-16.440	44.156	-12.497	-96.051
2.50000	-4.484	178.920	6.366	70.688	-15.232	44.695	-12.732	-101.516
3.00000	-4.529	173.119	4.936	64.815	-14.167	44.362	-12.656	-106.420
3.50000	-4.571	168.128	3.761	59.454	-13.235	43.396	-12.422	-110.949
4.00000	-4.611	163.682	2.776	54.501	-12.422	41.993	-12.114	-115.192
4.50000	-4.649	159.633	1.938	49.896	-11.714	40.296	-11.778	-119.197
5.00000	-4.684	155.892	1.215	45.600	-11.096	38.407	-11.440	-122.995
5.50000	-4.717	152.402	0.587	41.585	-10.556	36.399	-11.114	-126.607
6.00000	-4.746	149.123	0.036	37.828	-10.083	34.323	-10.807	-130.048

TABLE III. - Continued.

(d) I_B = 0.321 mA, I_C 17 mA

FREQ-GHZ	DB[S11] NASAHBT	ANG[S11] NASAHBT	DB[S21] NASAHBT	ANG[S21] NASAHBT	DB[S12] NASAHBT	ANG[S12] NASAHBT	DB[S22] NASAHBT	ANG[S22] NASAHBT
0.500000	-4.617	-128.066	20.099	109.814	-22.897	47.294	-7.163	-74.937
1.00000	-4.968	-157.777	14.735	93.105	-20.294	49.998	-11.502	-95.166
1.50000	-5.063	-171.061	11.408	84.004	-18.136	53.175	-13.415	-106.167
2.00000	-5.113	-179.607	9.050	77.095	-16.317	54.312	-14.200	-113.666
2.50000	-5.152	173.857	7.254	71.178	-14.802	54.011	-14.415	-119.354
3.00000	-5.188	168.387	5.823	65.852	-13.534	52.827	-14.335	-124.030
3.50000	-5.224	163.574	4.652	60.950	-12.466	51.106	-14.105	-128.117
4.00000	-5.258	159.215	3.673	56.389	-11.557	49.061	-13.803	-131.846
4.50000	-5.291	155.196	2.843	52.123	-10.779	46.826	-13.475	-135.341
5.00000	-5.322	151.451	2.131	48.121	-10.109	44.486	-13.143	-138.669
5.50000	-5.350	147.935	1.514	44.363	-9.528	42.099	-12.822	-141.866
6.00000	-5.374	144.619	0.975	40.827	-9.024	39.703	-12.518	-144.953
6.50000	-5.394	141.479	0.501	37.499	-8.584	37.323	-12.234	-147.942
7.00000	-5.409	138.499	0.082	34.363	-8.198	34.978	-11.973	-150.837
7.50000	-5.420	135.665	-0.292	31.403	-7.860	32.680	-11.732	-153.646
8.00000	-5.425	132.964	-0.626	28.607	-7.564	30.435	-11.512	-156.370

(e) I_B = 0.457 mA, I_C = 25.0 mA

FREQ-GHZ	DB[S11] NASAHBT	ANG[S11] NASAHBT	DB[S21] NASAHBT	ANG[S21] NASAHBT	DB[S12] NASAHBT	ANG[S12] NASAHBT	DB[S22] NASAHBT	ANG[S22] NASAHBT
0.500000	-4.277	-137.205	20.540	107.094	-23.795	45.686	-7.948	-85.750
1.00000	-4.413	-163.065	15.036	91.828	-21.202	50.136	-11.945	-109.792
1.50000	-4.454	-174.615	11.673	83.421	-18.988	53.956	-13.489	-122.544
2.00000	-4.484	177.785	9.297	76.946	-17.127	55.422	-14.051	-130.366
2.50000	-4.513	171.841	7.485	71.340	-15.578	55.351	-14.167	-135.631
3.00000	-4.543	166.773	6.041	66.253	-14.282	54.354	-14.061	-139.531
3.50000	-4.575	162.248	4.855	61.538	-13.186	52.795	-13.842	-142.691
4.00000	-4.608	158.100	3.862	57.126	-12.252	50.894	-13.568	-145.452
4.50000	-4.641	154.239	3.017	52.978	-11.449	48.786	-13.270	-147.995
5.00000	-4.674	150.611	2.290	49.069	-10.754	46.556	-12.968	-150.418
5.50000	-4.705	147.181	1.658	45.381	-10.149	44.264	-12.673	-152.771
6.00000	-4.733	143.926	1.105	41.899	-9.620	41.949	-12.389	-155.079
6.50000	-4.759	140.830	0.617	38.609	-9.157	39.638	-12.122	-157.355
7.00000	-4.782	137.879	0.183	35.499	-8.749	37.348	-11.872	-159.601
7.50000	-4.800	135.061	-0.204	32.557	-8.389	35.094	-11.639	-161.820
8.00000	-4.815	132.369	-0.552	29.771	-8.071	32.884	-11.424	-164.008
8.50000	-4.825	129.793	-0.866	27.129	-7.790	30.723	-11.225	-166.164

TABLE III. – Concluded.

(f) I_B = 0.6536 mA, I_C = 35 mA

FREQ-GHZ	DB[S11] NASAHBT	ANG[S11] NASAHBT	DB[S21] NASAHBT	ANG[S21] NASAHBT	DB[S12] NASAHBT	ANG[S12] NASAHBT	DB[S22] NASAHBT	ANG[S22] NASAHBT
0.500000	-4.629	-140.239	20.850	105.327	-24.437	48.663	-8.703	-84.987
1.00000	-4.779	-164.913	15.276	90.780	-21.386	54.549	-12.900	-106.729
1.50000	-4.823	-176.040	11.902	82.633	-18.891	57.983	-14.539	-118.487
2.00000	-4.854	176.535	9.524	76.274	-16.881	58.837	-15.127	-125.924
2.50000	-4.883	170.664	7.716	70.727	-15.250	58.231	-15.225	-131.107
3.00000	-4.913	165.620	6.276	65.671	-13.905	56.804	-15.081	-135.091
3.50000	-4.945	161.090	5.097	60.974	-12.779	54.903	-14.817	-138.435
4.00000	-4.978	156.924	4.111	56.572	-11.825	52.725	-14.497	-141.435
4.50000	-5.011	153.036	3.274	52.430	-11.008	50.388	-14.157	-144.248
5.00000	-5.042	149.378	2.555	48.526	-10.303	47.969	-13.816	-146.955
5.50000	-5.073	145.918	1.931	44.841	-9.691	45.517	-13.487	-149.594
6.00000	-5.101	142.634	1.386	41.363	-9.158	43.064	-13.175	-152.186
6.50000	-5.126	139.511	0.906	38.077	-8.690	40.633	-12.883	-154.738
7.00000	-5.147	136.535	0.480	34.970	-8.279	38.239	-12.611	-157.250
7.50000	-5.164	133.697	0.100	32.031	-7.917	35.892	-12.360	-159.723
8.00000	-5.177	130.988	-0.240	29.247	-7.598	33.599	-12.129	-162.154
8.50000	-5.186	128.399	-0.546	26.608	-7.315	31.364	-11.917	-164.543

TABLE IV.   MEASURED AND MODELED G_{max} AND   K

$[V_{CE} = 5.0$ V.]

(a) I_B = 0.053 mA, I_C = 2.0 mA

FREQ-GHZ	DB[GMAX] TRW	DB[GMAX] NASAHBT	K TRW	K NASAHBT
0.500000	15.879	15.527	0.363	0.249
1.00000	12.973	12.394	0.581	0.471
1.50000	11.365	10.462	0.788	0.650
2.00000	10.245	9.024	0.994	0.784
2.50000	7.122	7.874	1.152	0.878
3.00000	5.074	6.921	1.396	0.942
3.50000	4.131	6.118	1.488	0.985
4.00000	3.235	4.765	1.589	1.012
4.50000	2.554	3.801	1.655	1.029
5.00000	1.788	3.116	1.745	1.040

(b) I_B = 0.0915 mA, I_C = 4.0 mA

FREQ-GHZ	DB[GMAX] TRW	DB[GMAX] NASAHBT	K TRW	K NASAHBT
0.500000	18.401	18.150	0.403	0.282
1.00000	15.386	14.963	0.654	0.533
1.50000	13.615	12.950	0.872	0.735
2.00000	10.705	11.414	1.067	0.886
2.50000	10.717	10.156	1.066	0.994
3.00000	6.691	7.515	1.385	1.067
3.50000	5.750	6.117	1.414	1.115
4.00000	4.806	5.074	1.463	1.145
4.50000	4.013	4.245	1.516	1.162
5.00000	3.332	3.566	1.520	1.172
5.50000	2.585	2.999	1.532	1.175
6.00000	1.819	2.518	1.560	1.175

(c) I_B = 0.193 mA, I_C = 9.25 mA

FREQ-GHZ	DB[GMAX] TRW	DB[GMAX] NASAHBT	K TRW	K NASAHBT
0.500000	20.741	19.987	0.408	0.330
1.00000	17.542	16.493	0.795	0.585
1.50000	15.536	14.136	0.993	0.751
2.00000	11.671	12.298	1.133	0.854
2.50000	9.679	10.799	1.241	0.917
3.00000	8.044	9.551	1.327	0.957
3.50000	6.892	8.498	1.350	0.982
4.00000	5.892	7.599	1.376	0.999
4.50000	5.018	6.208	1.403	1.010
5.00000	4.355	5.344	1.383	1.018
5.50000	3.724	4.652	1.372	1.023
6.00000	3.107	4.073	1.369	1.026

TABLE IV. - Continued.

(d) $I_B = 0.321$ mA, $I_C = 17$ mA

FREQ-GHZ	DB[GMAX] TRW	DB[GMAX] NASAHBT	K TRW	K NASAHBT
0.500000	22.326	21.498	0.590	0.470
1.00000	18.907	17.514	0.902	0.743
1.50000	14.685	14.772	1.094	0.874
2.00000	11.844	12.684	1.216	0.939
2.50000	10.007	11.028	1.282	0.973
3.00000	8.293	9.679	1.364	0.993
3.50000	7.392	8.126	1.310	1.005
4.00000	6.411	6.930	1.319	1.012
4.50000	5.490	6.005	1.515	1.017
5.00000	4.833	5.243	1.323	1.020
5.50000	4.203	4.600	1.305	1.023
6.00000	3.574	4.049	1.307	1.024
6.50000	3.157	3.571	1.282	1.025
7.00000	2.624	3.154	1.293	1.026
7.50000	2.072	2.787	1.332	1.026
8.00000	2.209	2.462	1.208	1.027

(e) $I_B = 0.457$ mA, $I_C = 25.0$ mA

FREQ-GHZ	DB[GMAX] TRW	DB[GMAX] NASAHBT	K TRW	K NASAHBT
0.500000	23.038	22.167	0.653	0.491
1.00000	19.394	18.119	0.965	0.765
1.50000	14.647	15.331	1.136	0.893
2.00000	12.001	13.212	1.227	0.954
2.50000	10.158	11.531	1.279	0.987
3.00000	8.515	9.715	1.337	1.005
3.50000	7.558	8.238	1.288	1.016
4.00000	6.604	7.125	1.289	1.023
4.50000	5.774	6.218	1.298	1.027
5.00000	5.046	5.457	1.287	1.030
5.50000	4.411	4.807	1.269	1.032
6.00000	3.760	4.245	1.273	1.033
6.50000	3.340	3.755	1.253	1.034
7.00000	2.871	3.324	1.253	1.035
7.50000	2.194	2.942	1.308	1.035
8.00000	2.439	2.602	1.181	1.036
8.50000	2.185	2.298	1.123	1.036

TABLE IV. - Concluded.

(f) $I_B = 0.6536$ mA, $I_C = 35$ mA

FREQ-GHZ	DB[GMAX] TRW	DB[GMAX] NASAHBT	K TRW	K NASAHBT
0.500000	23.502	22.644	0.711	0.556
1.00000	18.838	18.331	1.020	0.816
1.50000	14.573	15.396	1.171	0.919
2.00000	11.996	13.203	1.245	0.965
2.50000	10.214	11.483	1.283	0.989
3.00000	8.694	9.892	1.309	1.001
3.50000	7.604	8.383	1.284	1.008
4.00000	6.680	7.286	1.280	1.012
4.50000	5.821	6.395	1.291	1.015
5.00000	5.076	5.648	1.283	1.016
5.50000	4.482	5.011	1.256	1.017
6.00000	3.815	4.460	1.266	1.018
6.50000	3.387	3.980	1.246	1.018
7.00000	2.906	3.558	1.248	1.018
7.50000	2.343	3.184	1.286	1.018
8.00000	2.438	2.851	1.185	1.018
8.50000	2.172	2.552	1.128	1.018

TABLE V. – MEASURED AND MODELED h_{21}

[V_{CE} = 5.0 V.]

(a) I_B = 0.053 mA, I_C = 2.0 mA

FREQ-GHZ	$\lvert h_{21}\rvert$[dB] TRW	$\underline{/}h_{21}$[Deg] TRW	$\lvert h_{21}\rvert$[dB] NASAHBT	$\underline{/}h_{21}$[Deg] NASAHBT
0.5	14.884	-86.897	15.388	-78.742
1.0	9.219	-94.296	9.798	-91.898
1.5	5.994	-99.705	6.587	-99.537
2.0	3.849	-103.807	4.449	-105.485
2.5	2.303	-107.479	2.931	-110.513
3.0	1.272	-111.323	1.817	-114.884
3.5	0.347	-114.683	0.986	-118.721

(b) I_B = 0.0915 mA, I_C = 4.0 mA

0.5	19.153	-84.055	19.329	-78.293
1.0	13.455	-92.895	13.651	-90.273
1.5	10.162	-98.973	10.324	-97.026
2.0	7.939	-103.601	8.040	-102.299
2.5	7.937	-103.684	6.354	-106.850
3.0	5.159	-112.033	5.059	-110.930
3.5	4.094	-115.961	4.039	-114.639
4.0	3.277	-119.692	3.225	-118.034
4.5	2.695	-123.078	2.568	-121.146
5.0	2.185	-126.982	2.036	-124.010
5.5	1.750	-130.932	1.601	-126.645
6.0	1.378	-133.679	1.247	-129.076

(c) I_B = 0.193 mA, I_C = 9.25 mA

0.5	22.197	-81.280	23.078	-85.361
1.0	17.643	-89.661	17.193	-93.533
1.5	14.246	-97.973	13.788	-98.815
2.0	11.801	-104.325	11.434	-103.288
2.5	10.149	-110.933	9.672	-107.366
3.0	8.757	-116.086	8.294	-111.167
3.5	7.506	-120.771	7.187	-114.746
4.0	6.566	-124.934	6.280	-118.125
4.5	5.718	-129.460	5.529	-121.315
5.0	4.959	-133.813	4.898	-124.327
5.5	4.247	-136.798	4.366	-127.173
6.0	3.564	-140.810	3.915	-129.859

TABLE V. Continued.

(d) $I_B = 0.321$ mA, $I_C = 17.0$ mA

FREQ-GHZ	$|h_{21}|$[dB] TRW	$\angle h_{21}$[Deg] TRW	$|h_{21}|$[dB] NASAHBT	$\angle h_{21}$[Deg] NASAHBT
0.5	25.121	-80.662	25.541	-82.094
1.0	19.445	-93.801	19.713	-93.085
1.5	16.108	-101.069	16.278	-99.855
2.0	13.662	-107.896	13.867	-105.434
2.5	11.879	-113.563	12.031	-110.423
3.0	10.483	-119.416	10.564	-115.006
3.5	9.042	-124.139	9.359	-119.258
4.0	7.997	-128.820	8.346	-123.214
4.5	7.141	-133.445	7.483	-126.895
5.0	6.231	-138.131	6.739	-130.316
5.5	5.455	-142.340	6.092	-133.492
6.0	4.888	-145.744	5.525	-136.436
6.5	4.230	-150.024	5.026	-139.165
7.0	3.623	-154.430	4.584	-141.698
7.5	3.151	-151.444	4.190	-144.045
8.0	2.854	-160.296	3.839	-146.221

(e) $I_B = 0.457$ mA, $I_C = 25$ mA

FREQ-GHZ	$|h_{21}|$[dB] TRW	$\angle h_{21}$[Deg] TRW	$|h_{21}|$[dB] NASAHBT	$\angle h_{21}$[Deg] NASAHBT
0.5	26.121	-80.741	26.066	-81.789
1.0	20.401	-94.765	20.239	-92.790
1.5	17.035	-102.260	16.795	-99.513
2.0	14.530	-109.579	14.373	-105.038
2.5	12.683	-115.529	12.522	-109.979
3.0	11.246	-121.504	11.040	-114.526
3.5	9.730	-126.131	9.815	-118.756
4.0	8.609	-131.177	8.783	-122.702
4.5	7.637	-135.648	7.898	-126.382
5.0	6.739	-140.457	7.132	-129.815
5.5	5.916	-144.492	6.462	-133.011
6.0	5.254	-147.562	5.872	-135.983
6.5	4.545	-152.065	5.350	-138.745
7.0	3.917	-155.901	4.884	-141.310
7.5	3.367	-157.334	4.468	-143.691
8.0	3.058	-161.940	4.095	-145.904
8.5	2.583	-167.381	3.758	-147.959

15

TABLE V. - Concluded.

(f) I_B = 0.6536 mA, I_C = 35 mA

FREQ-GHZ	$\|h_{21}\|$[dB] TRW	$\angle h_{21}$[Deg] TRW	$\|h_{21}\|$[dB] NASAHBT	$\angle h_{21}$[Deg] NASAHBT
0.5	26.724	-80.493	26.442	-82.706
1.0	20.994	-95.103	20.594	-93.674
1.5	17.594	-102.941	17.139	-100.546
2.0	15.066	-110.496	14.703	-106.255
2.5	13.144	-117.459	12.838	-111.377
3.0	11.529	-127.842	11.338	-116.086
3.5	10.145	-127.701	10.096	-120.456
4.0	8.986	-132.549	9.046	-124.516
4.5	7.973	-137.340	8.143	-128.287
5.0	7.031	-142.011	7.358	-131.782
5.5	6.189	-144.835	6.670	-135.021
6.0	5.449	-149.357	6.064	-138.013
6.5	4.709	-153.472	5.525	-140.780
7.0	4.049	-157.143	5.044	-143.332
7.5	3.550	-158.160	4.614	-145.687
8.0	3.180	-163.041	4.228	-147.863
8.5	2.630	-167.849	3.880	-149.877

16
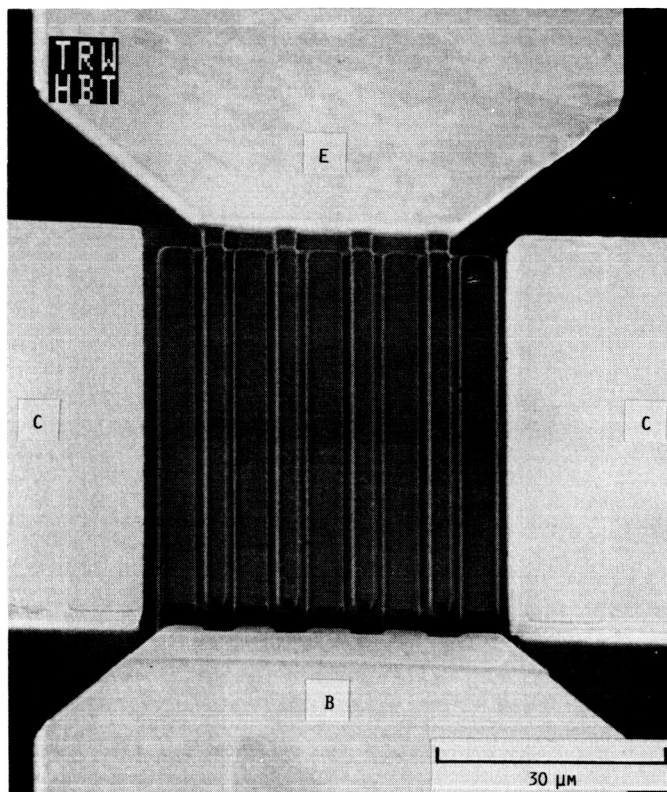
(A) SEM PICTURE OF THE TRW EMITTER-UP NPN AlGaAs/GaAs HETEROJUNCTION
BIPOLAR TRANSISTOR (HBT) ILLUSTRATING THE INTERDIGITATED EMITTER-
BASE REGION.
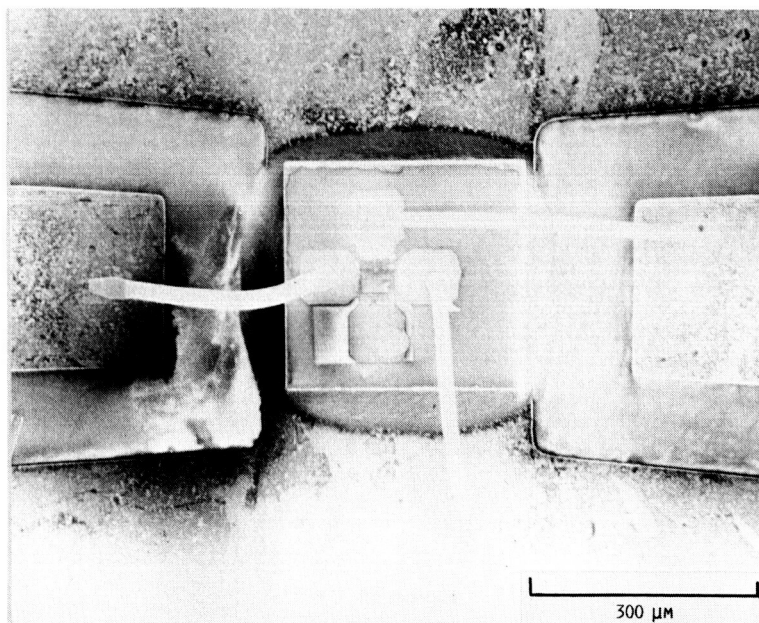
(B) HBT MOUNTED ON AND WIRE BONDED TO THE COPLANAR-WAVEGUIDE ALUMINA CARRIER IN
THE COMMON EMITTER CONFIGURATION.

FIGURE 1. - SEM PICTURE OF THE DISCRETE TRW HBT DEVICE.
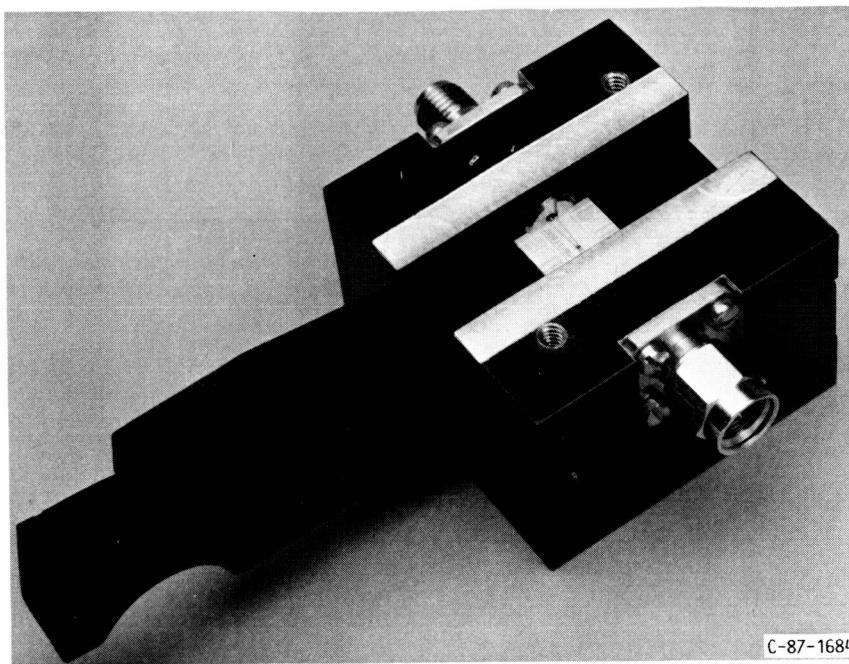
(A) TEST FIXTURE.
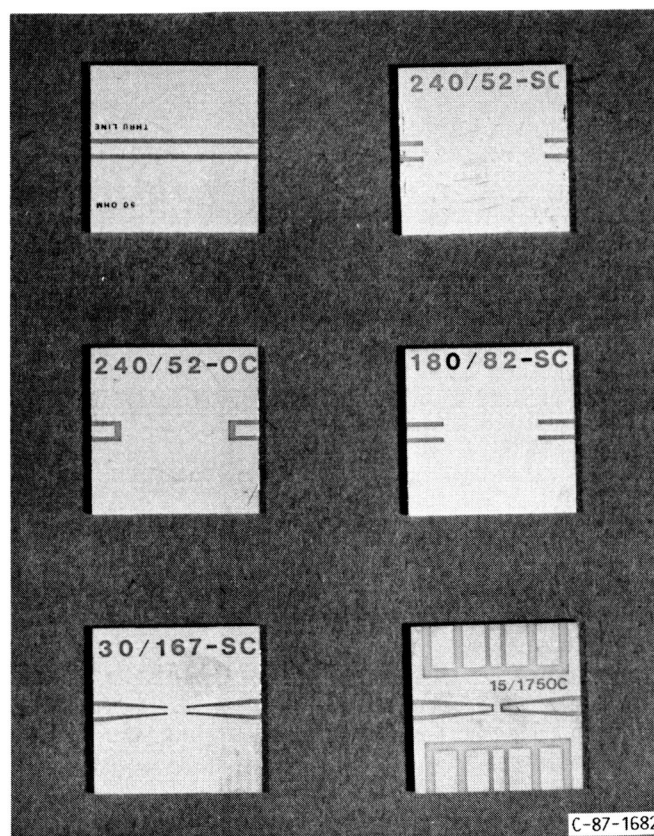
(B) CALIBRATION KIT.

FIGURE 2. - DESIGN TECHNIQUE COPLANAR WAVEGUIDE APPARATUS.
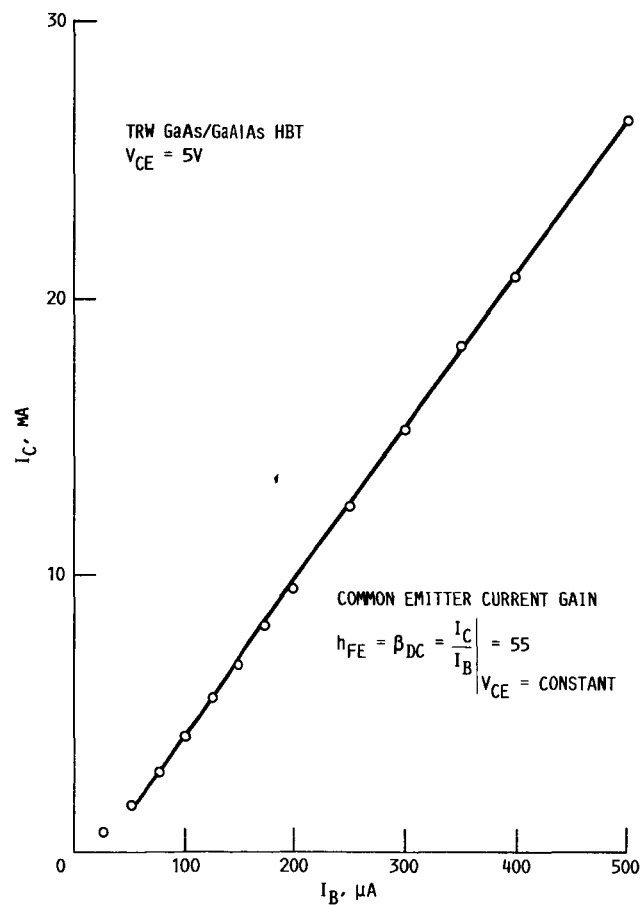
FIGURE 3. - COLLECTOR CURRENT VERSUS THE BASE CURRENT FOR A
FIXED COLLECTOR-TO-EMITTER VOLTAGE.

19
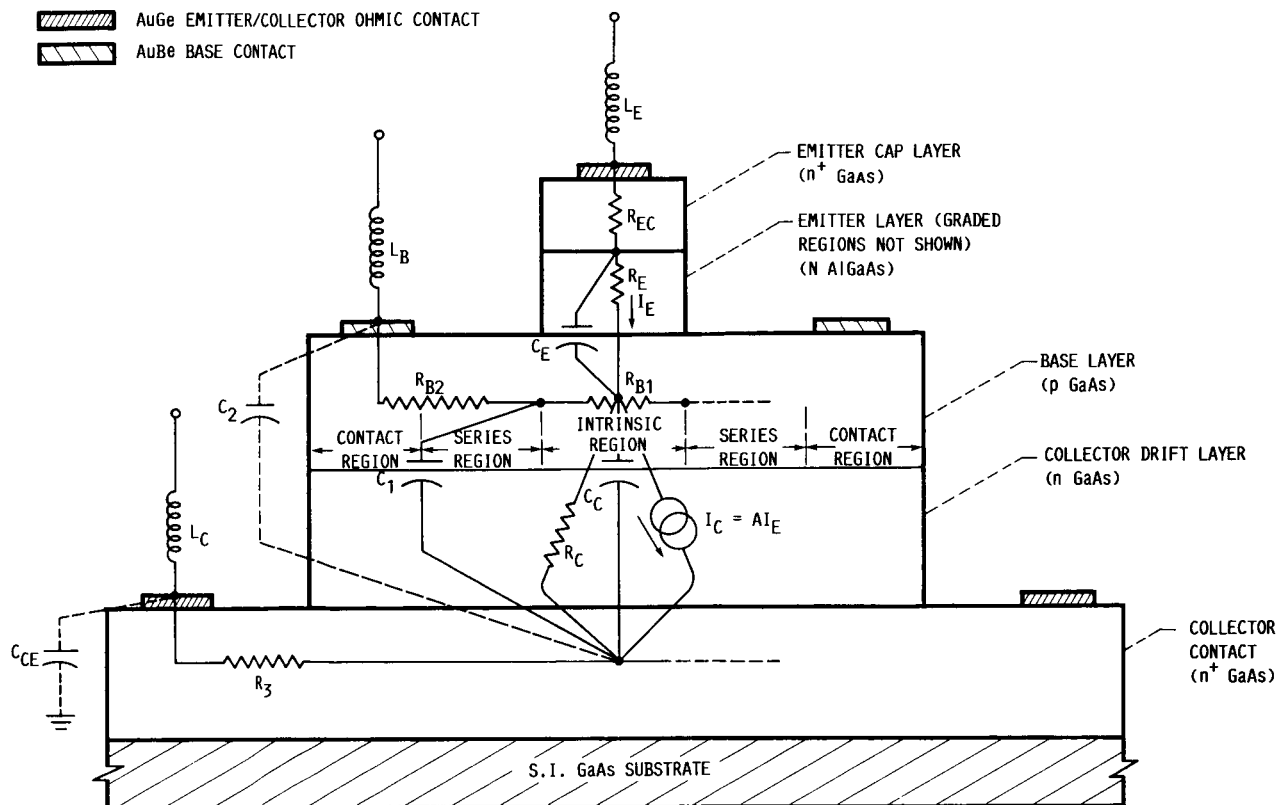
FIGURE 4. - SCHEMATIC CROSS SECTION OF THE HBT SHOWING THE ORIGIN OF EACH LUMPED ELEMENT IN THE SMALL SIGNAL CE EQUIVALENT CIRCUIT MODEL.
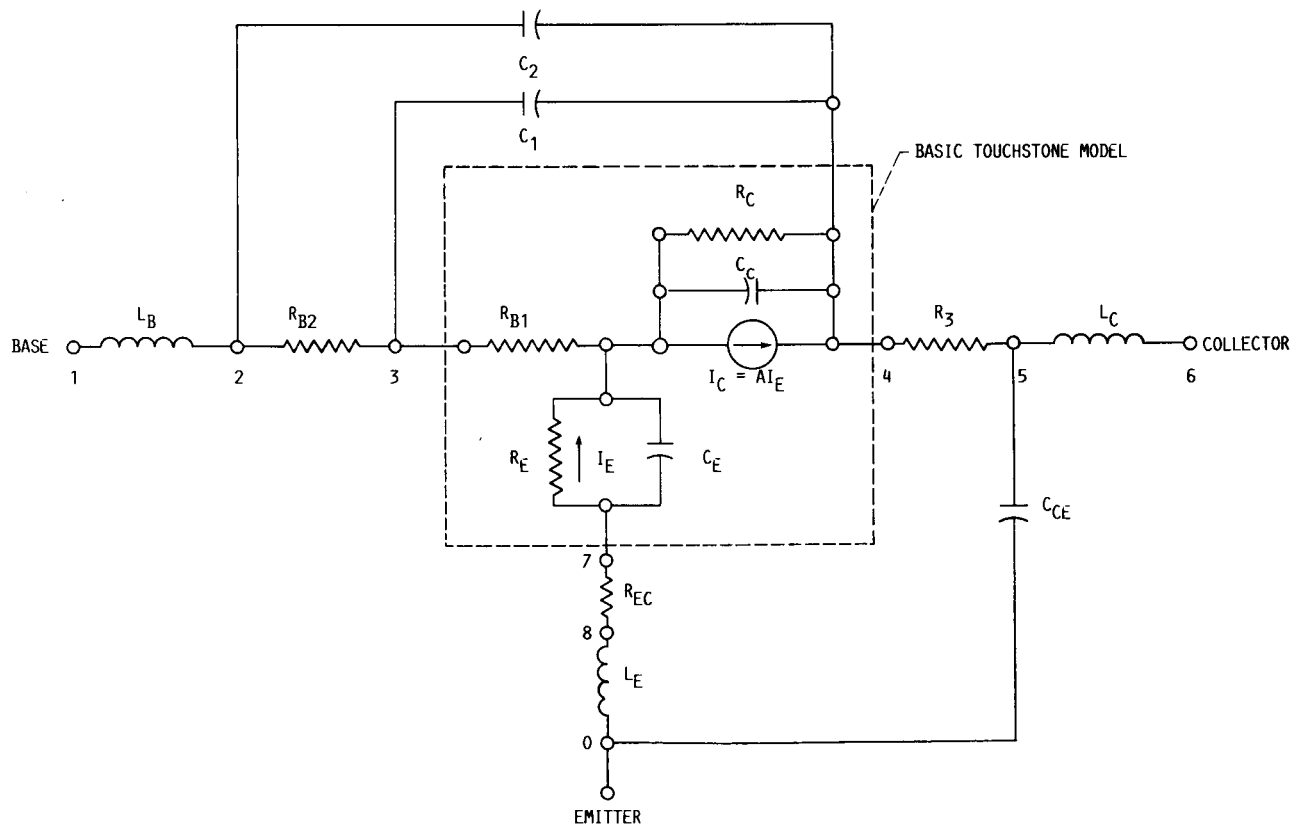
FIGURE 5. - COMMON EMITTER SMALL SIGNAL LUMPED ELEMENT EQUIVALENT CIRCUIT MODEL OF A MICROWAVE GaAs/GaAlAs HETEROJUNCTION BIPOLAR TRANSISTOR.

20
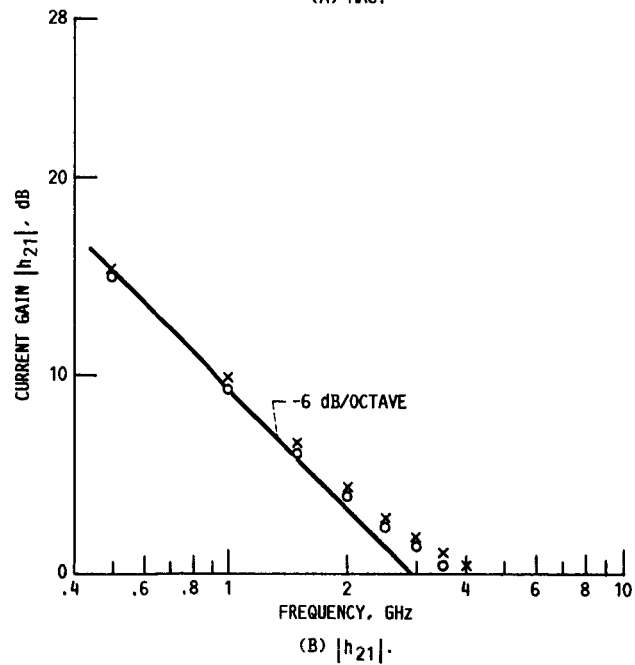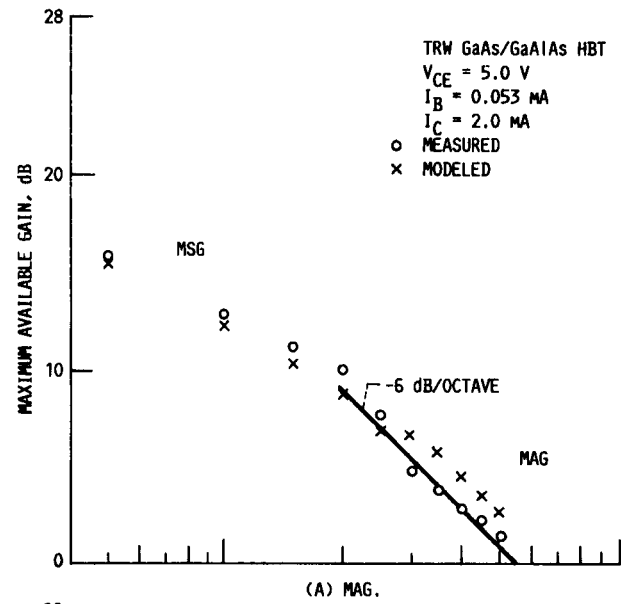
FIGURE 6. - MEASURED AND MODELED PARAMETERS FOR
I_C = 2.0 MA.

21

$f_1 = 0.500000$
$f_2 = 5.000000$

☐ S_{11} TRW
\+ S_{22} TRW
✳ S_{11} NASA HBT
✕ S_{22} NASA HBT

(C) S_{11}, S_{22}.

☐ dB[S_{21}] TRW
\+ dB[S_{12}] TRW
✳ dB[S_{21}] NASA HBT
✕ dB[S_{12}] NASA HBT

FREQUENCY, GHz
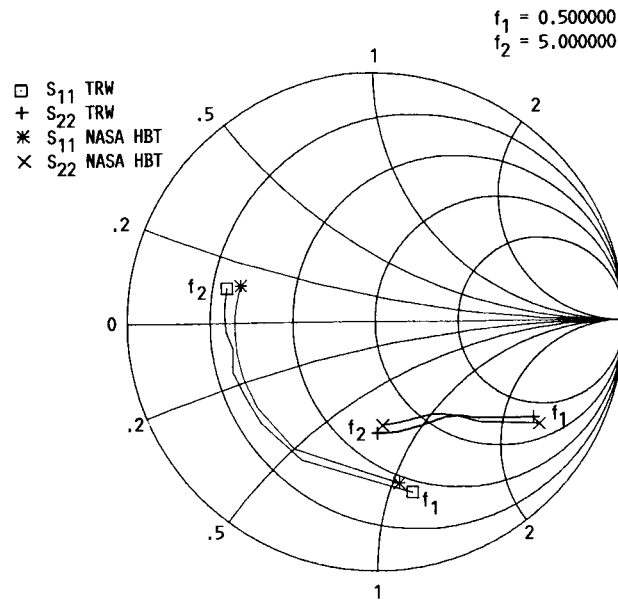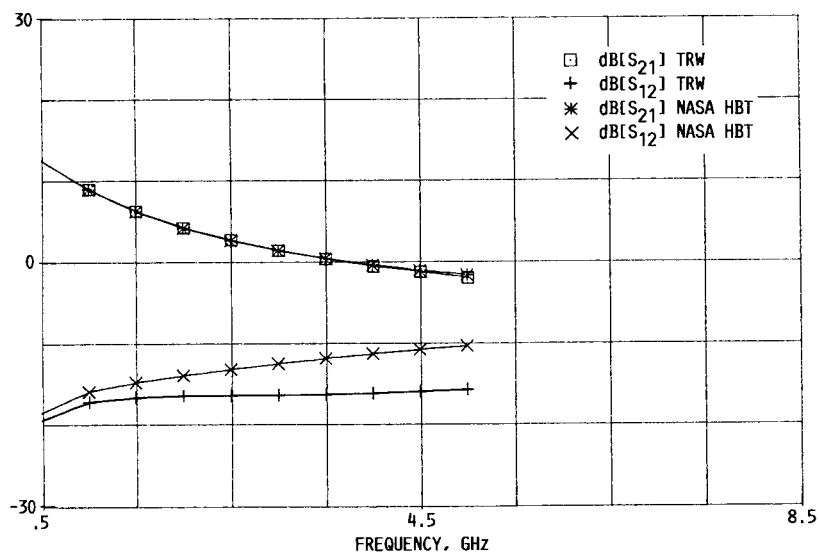
(D) S_{12}, S_{21}.

FIGURE 6. - CONCLUDED.

22
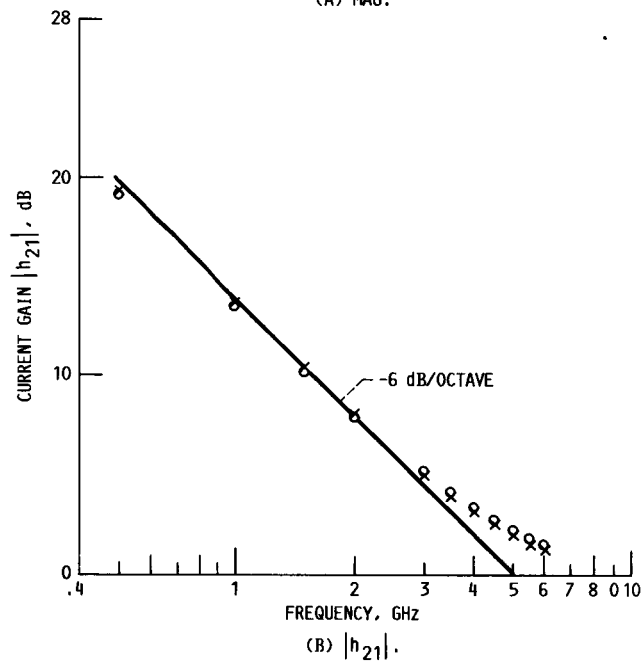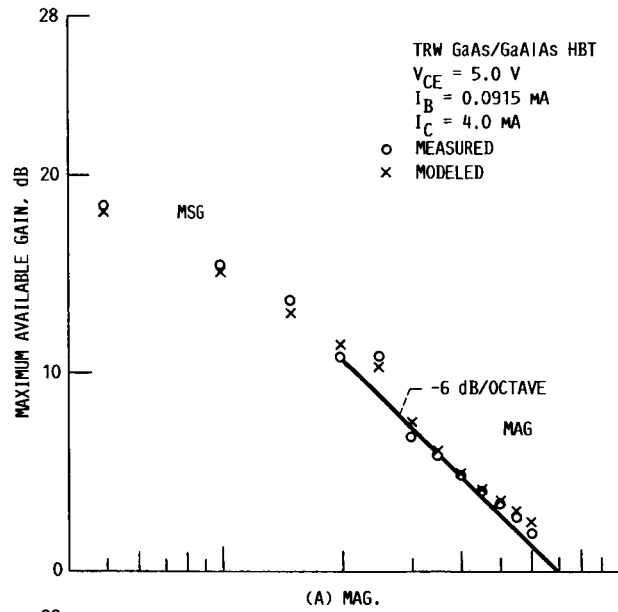
FIGURE 7. – MEASURED AND MODELED PARAMETERS FOR
I_C = 4.0 MA.

23

$f_1 = 0.500000$
$f_2 = 6.000000$

☐ S_{11} TRW
+ S_{22} TRW
✳ S_{11} NASA HBT
✕ S_{22} NASA HBT

(C) S_{11}, S_{22}.

☐ dB[S_{21}] TRW
+ dB[S_{12}] TRW
✳ dB[S_{21}] NASA HBT
✕ dB[S_{12}] NASA HBT

FREQUENCY, GHz
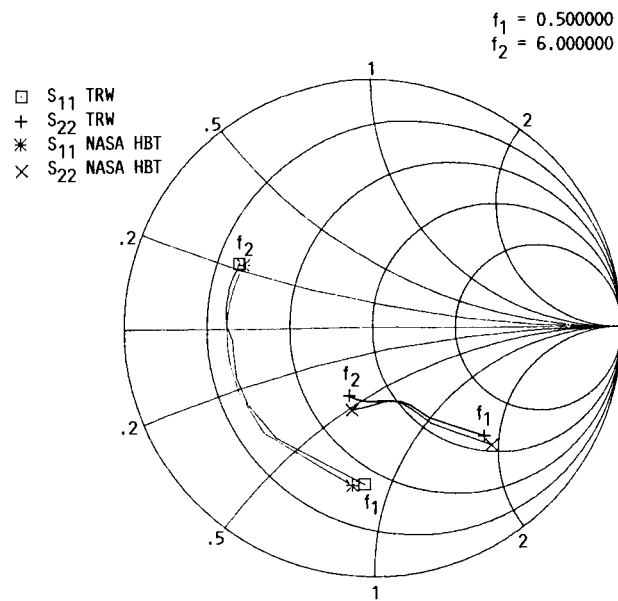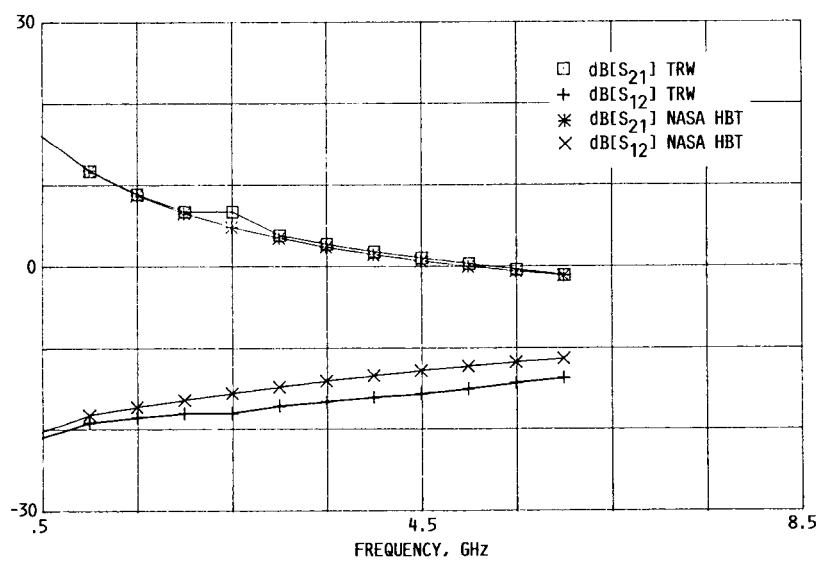
(D) S_{12}, $S21$.

FIGURE 7. - CONCLUDED.

24
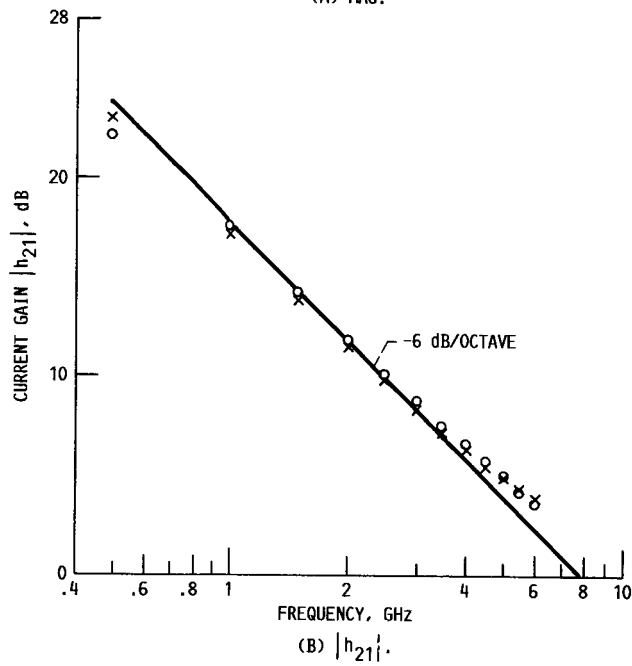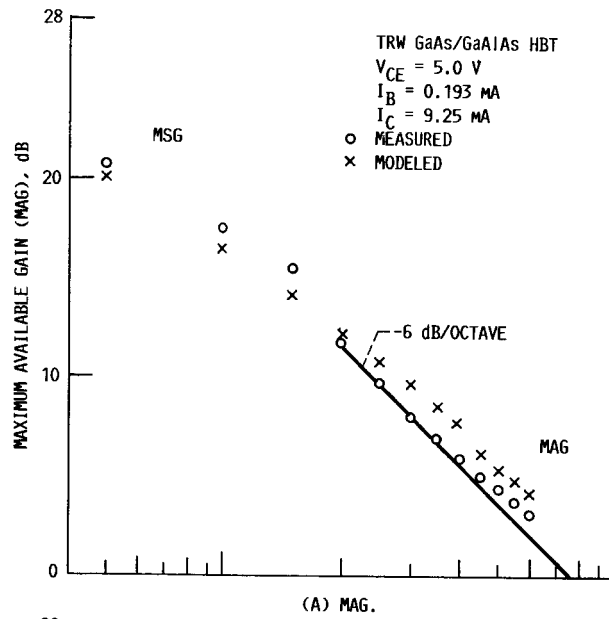
FIGURE 8. – MEASURED AND MODELED PARAMETERS FOR
I_C = 9.25 mA.

f₁ = 0.500000
f₂ = 6.00000
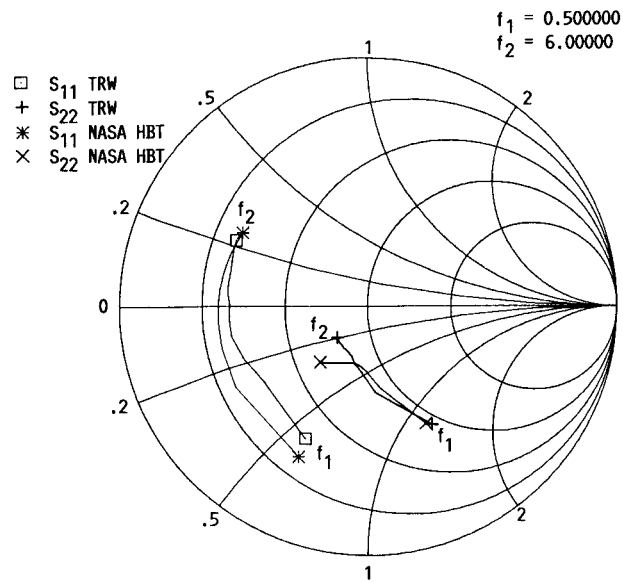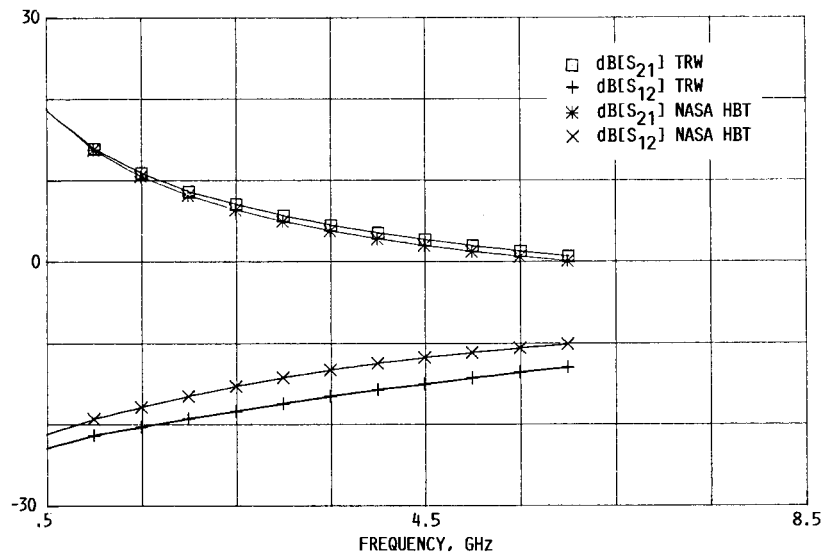
(C) S_{11}, S_{22}.

(D) S_{12}, S_{21}.

FIGURE 8. – CONCLUDED.
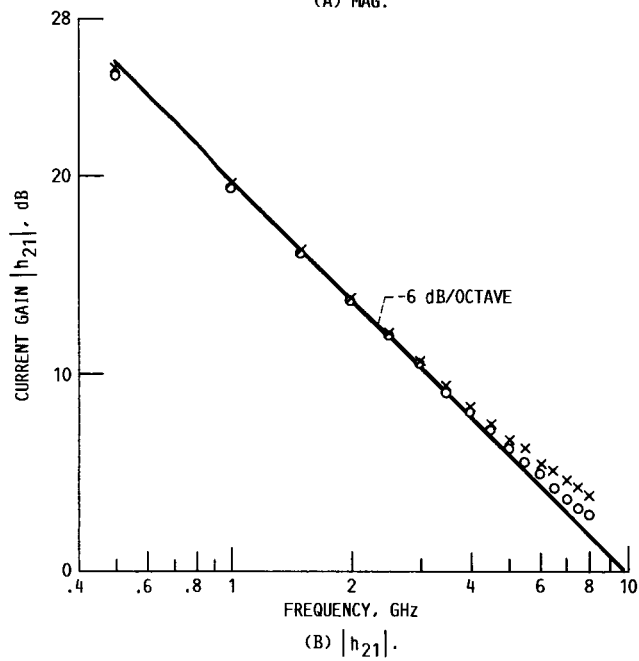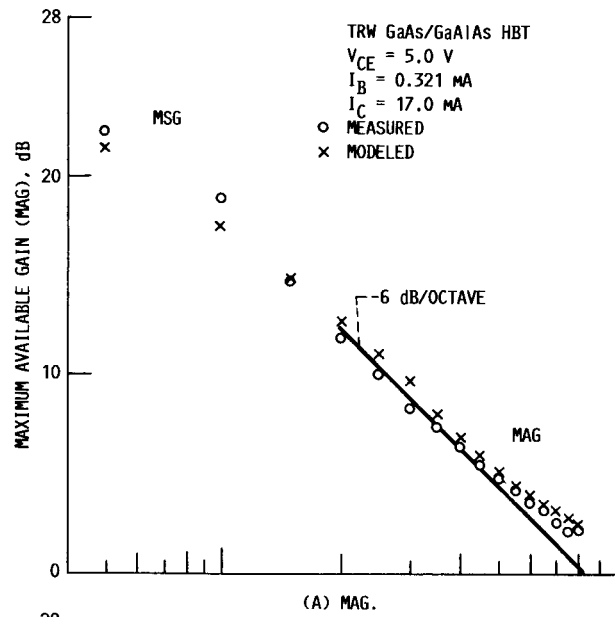
FIGURE 9. - MEASURED AND MODELED PARAMETERS FOR
I_C = 17 MA.

27

f_1 = 0.500000
f_2 = 8.000000

□ S_{11} TRW
+ S_{22} TRW
✳ S_{11} NASA HBT
✕ S_{22} NASA HBT

(C) S_{11}, S_{22}.

□ $dB[S_{21}]$ TRW
+ $dB[S_{12}]$ TRW
✳ $dB[S_{21}]$ NASA HBT
✕ $dB[S_{12}]$ NASA HBT

FREQUENCY, GHz
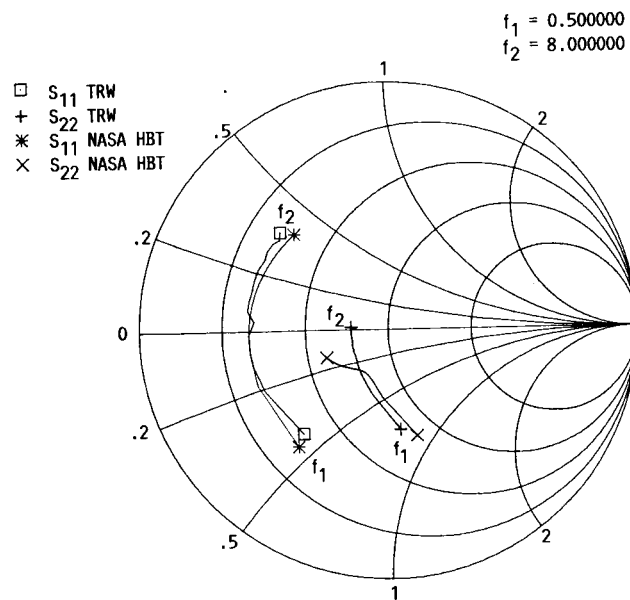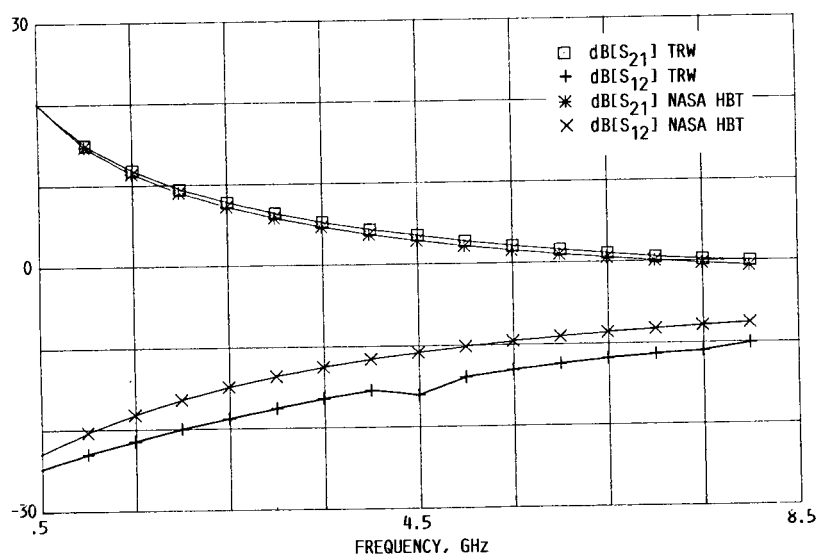
(D) S_{12}, S_{21}.

FIGURE 9. - CONCLUDED.
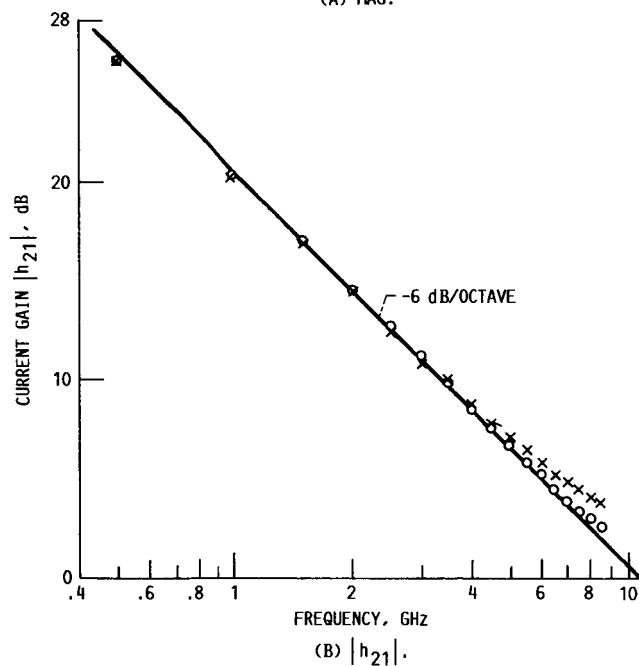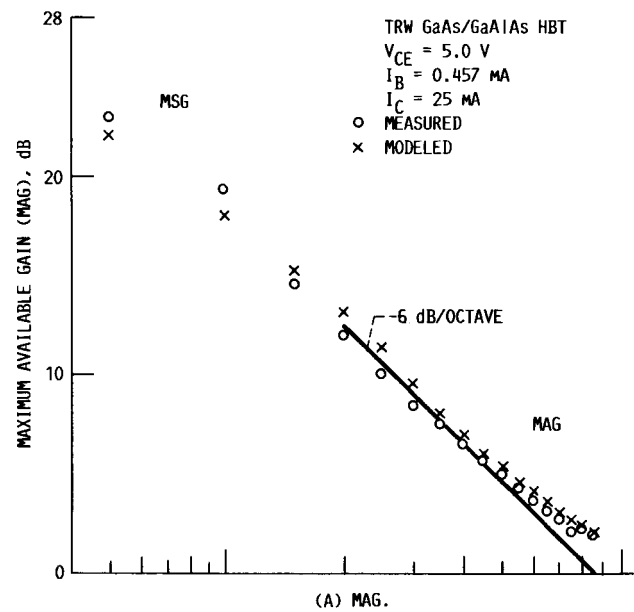
FIGURE 10. - MEASURED AND MODELED PARAMETERS FOR
I_C = 25 MA.

29

f_1 = 0.500000
f_2 = 8.500000

□ S_{11} TRW
+ S_{22} TRW
＊ S_{11} NASA HBT
✕ S_{22} NASA HBT

(C) S_{11}, S_{22}.

□ dB[S_{21}] TRW
+ dB[S_{12}] TRW
＊ dB[S_{21}] NASA HBT
✕ dB[S_{12}] NASA HBT

FREQUENCY, GHz
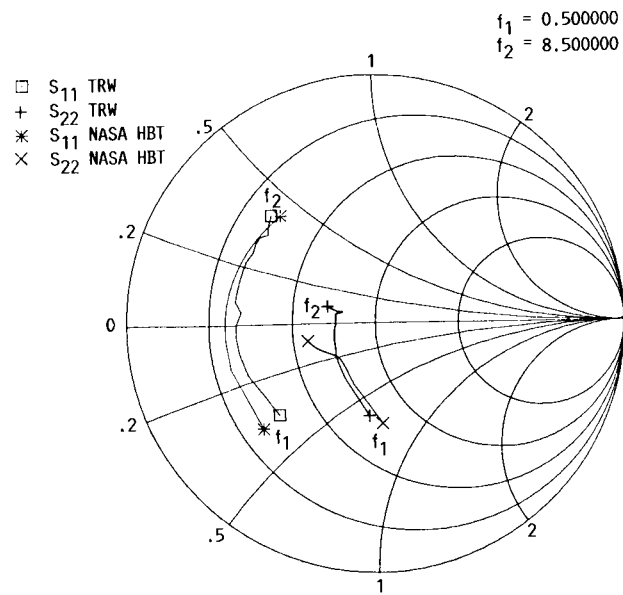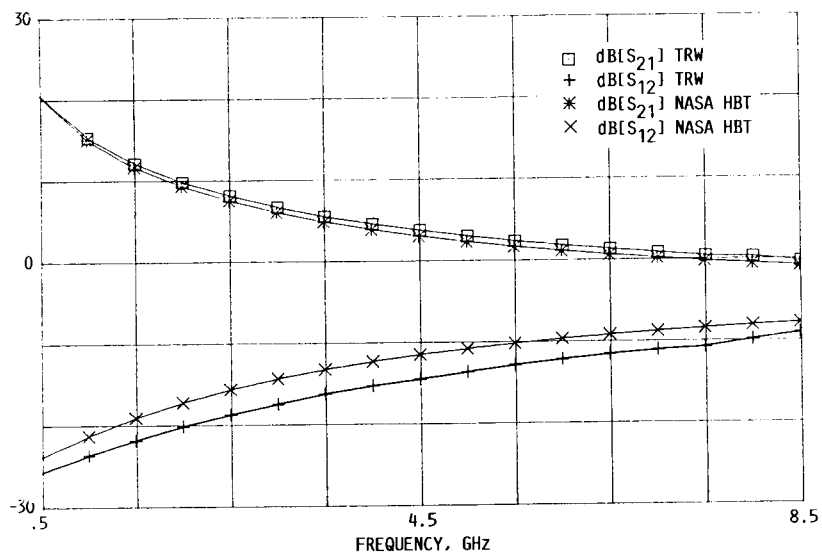
(D) S_{12}, S_{21}.

FIGURE 10. - CONCLUDED.

30
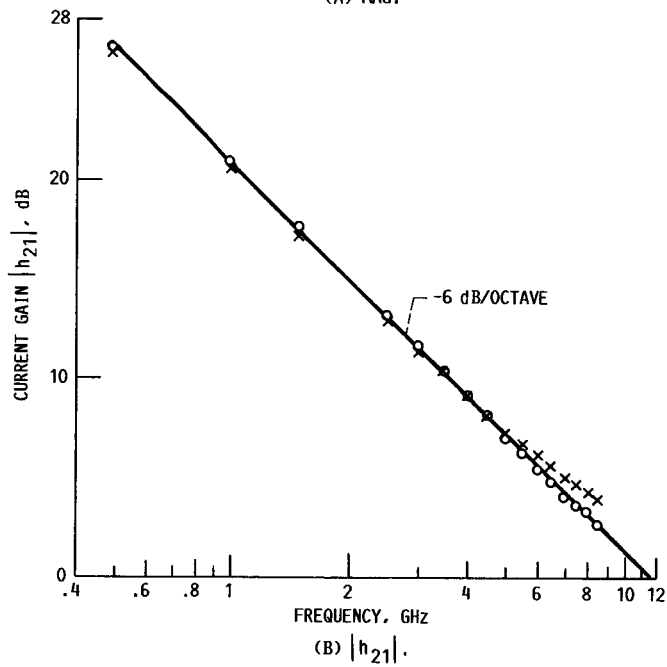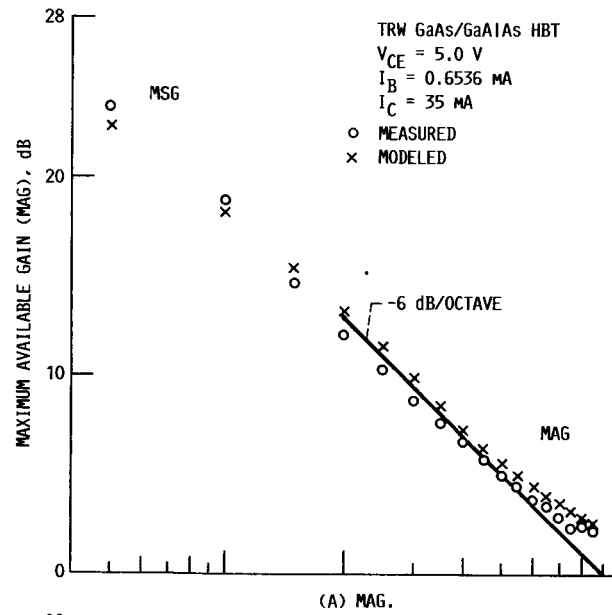
FIGURE 11. - MEASURED AND MODELED PARAMETERS FOR I_C = 35 mA.

□ S_{11} TRW
+ S_{22} TRW
✳ S_{11} NASA HBT
✕ S_{22} NASA HBT

(C) S_{11}, S_{22}.

FREQUENCY, GHz

□ dB[S_{21}] TRW
+ dB[S_{12}] TRW
✳ dB[S_{21}] NASA HBT
✕ dB[S_{12}] NASA HBT
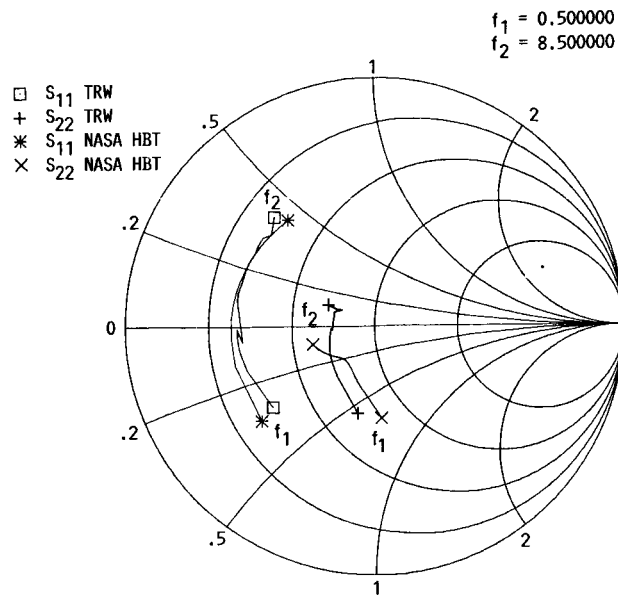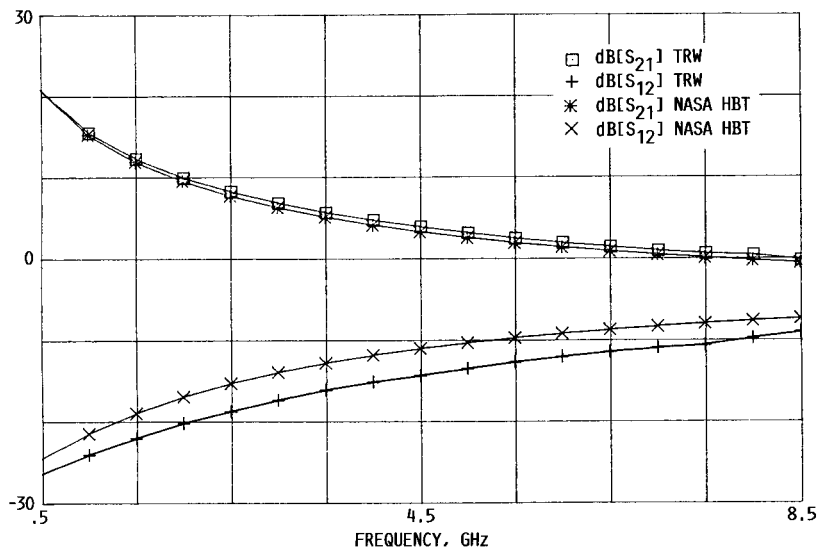
(D) S_{12}, S_{21}.

FIGURE 11. – CONCLUDED.

UNITY CURRENT GAIN CUTOFF FREQUENCY, f_T

MAXIMUM FREQUENCY OF OSCILLATION f_{MAX}

TRW GaAs/GaAlAs HBT
V_{CE} = 5.0 V

GHz

COLLECTOR CURRENT, I_C, MA
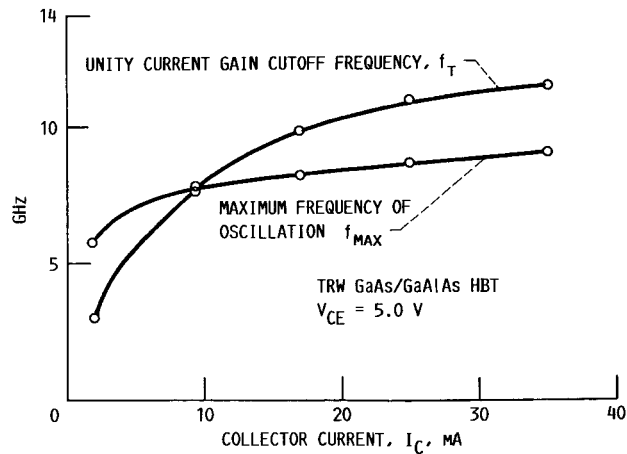
FIGURE 12.- f_{MAX} AND f_T AS A FUNCTION OF THE COLLECTOR CURRENT.

16. Abstract

The characterization and modeling of a microwave GaAs/AlGaAs heterojunction
Bipolar Transistor (HBT) are discussed. The de-embedded scattering parameters
are used to derive a small signal lumped element equivalent circuit model using
EEsof's "Touchstone" software package. Each element in the equivalent circuit
model is shown to have its origin within the device. The model shows good agree-
ment between the measured and modeled scattering parameters over a wide range of
bias currents. Further, the MAG and $|h_{21}|$ calculated from the measured data
and the MAG and $|h_{21}|$ predicted by the model are also in good agreement.
Consequently the model should also be capable of predicting the f_{max} and f_T of
other HBTs.